

CHAPTER V

Experimental Studies in the Vicinity of the C*-I* Transition

5.1 Introduction

It was stated earlier that all tilted smectic phases composed of chiral molecules exhibit ferroelectric properties. Results described hitherto (Chapter II to IV) are on the least ordered tilted smectic phase, viz., the smectic C* (C*) phase. Other tilted, but more ordered smectic phases,^{1,2} whose constituent molecules are optically active also exhibit ferroelectric properties. In all, seven chiral tilted smectic phases are known to date - SmC*, SmI*, SmF*, SmG*, SmH*, SmJ* and SmK*. All of them have, along with lamellar ordering, an additional ordering, viz., bond-orientational order (BOO). Since the tilt breaks the axial symmetry, even the C* phase possesses BOO, albeit of small magnitude.^{3,4} The I* and F* have enhanced BOO as compared with C*. They are both *hexatic* phases, the difference being that in the I* phase the molecular tilt is towards the apex of the hexagon (of the basal plane) while in F* it is towards the side of the hexagon. The remaining four phases G*, H*, J* and K* possess three dimensional long range positional order as in a crystal, besides

BOO. However, the interlayer ordering in these crystalline phases is very weak and therefore by convention they are generally described as smectic liquid crystals.

Since C* and I* have the same symmetry, the transition between them can only be first order.⁵ The other possibility is that I* can evolve continuously from C* without undergoing a phase transition. Clearly, it is of great interest to investigate how the nature of the transformation from C* to I* is reflected in the ferroelectric properties. In this chapter, we present measurements of the tilt angle θ , spontaneous polarization P_s , the static dielectric constant ϵ_{\perp} and the rotational viscosity γ_{ϕ} on two compounds which exhibit both C* and I* phases. Our results show that the temperature variation of the primary order parameter θ is reflected in the temperature variations of P_s and ϵ_{\perp} as well. Thus these studies allow a comparison of the nature of the $P_s - \theta$ coupling (which is, in the C* phase, an essential feature of the ferroelectric properties⁶) in the two phases.

5.2 Experimental

5.2.1 Materials

For our studies we have selected two compounds 8SI* and 8OSI* both of which exhibit C*-I* transition.⁷ The molecular structure and the phase sequence exhibited by these two compounds are given in Fig.5.1. As seen from the molecular structure both these compounds are esters with a phenyl 4-biphenyl-4'-carboxylate central core. The only notable difference in their structures is that 8SI* has an alkyl group while 8OSI* has an alkoxy group. An important reason for the selection of these two compounds is that in 8SI* the C*-I* transition is first order and in 8OSI* the I* phase evolves continuously from the C* phase. (These are confirmed by our X-ray experiments which will be discussed later.)

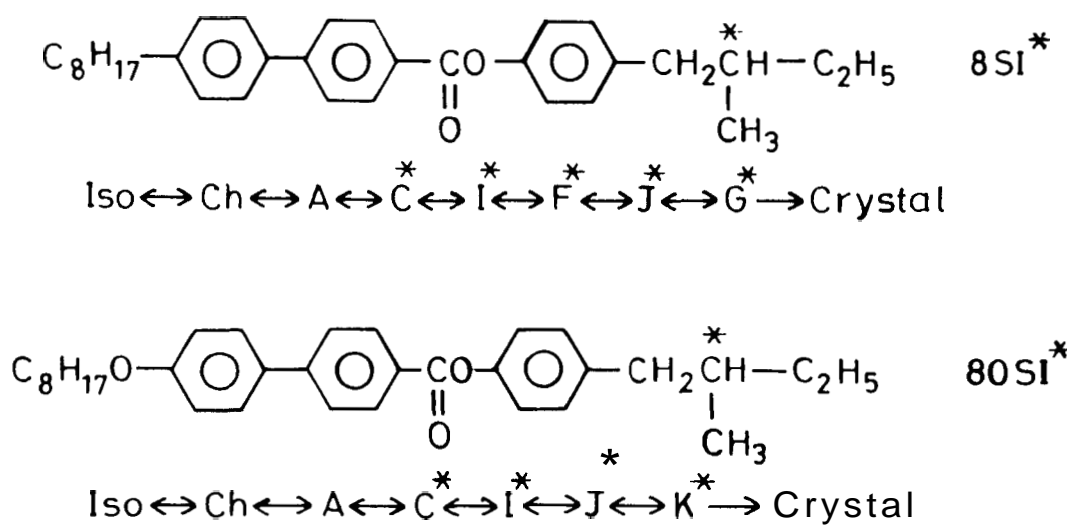


Fig.5.1. Molecular structure and phase sequence exhibited by the compounds used.

5.2.2 Temperature control and measurement

The experiments were carried out using a programmable hot stage (Mettler FP82) and a central processing unit (Mettler SO). The sample temperature was directly monitored using a bead thermistor having a high resistance and large temperature coefficient (YSI 44011) which was placed inside the hot stage adjacent to the sample cell. The thermistor resistance was measured in the four probe configuration by a digital multimeter (Keithley 195A).

5.2.3 Measurement of P_s

The calibrated Diamant bridge⁸ described in chapter II was used to obtain the hysteresis loop from which P_s and γ_ϕ were determined as described in chapters II and IV respectively.

In comparison to C* phase, in the higher ordered I* phase, one can expect the electric field necessary for the measurement to be large. For this purpose the output of the function generator was amplified by a high fidelity high voltage amplifier (Kepco BOP1000M).

5.2.4 Measurement of tilt angle

The tilt angle θ were measured by X-ray diffraction method. The details of the set-up and experimental procedure have been described already in Chapter II.

5.2.5 Measurement of static dielectric constant

The dielectric constant was measured by measuring the capacitance of the sample using an impedance analyser (HP4192A). The preparation of the sample cell, alignment of the sample and the data acquisition, storing and analysis were already

explained in Chapter III.

5.3 Results and Discussion

5.3.1 Tilt angle measurements

Figures 5.2 and 5.3 are the plots of tilt angle versus temperature for 8SI* and 8OSI* respectively. In the case of 8SI*, as seen from fig. 5.2, the tilt angle jumps abruptly across the C*-I* transition accompanied by a two phase co-existence region. This clearly indicates that the transition is first order. On the other hand, in 8OSI* the tilt angle decreases continuously across the C*-I* phase transition without any jump (see fig. 5.3) and without a co-existence region. According to the theory⁵ C*-I* transition can be either first order or I* can evolve continuously from the C* phase. In 8OSI* the absence of a jump in the tilt angle and the coexistence region, within the experimental limits, confirms that C*-I* transition is not first order and that I* phase evolves continuously from the C* phase. This result is in agreement with the high resolution X-ray studies of Brock et al.³, on the racemic form of the 8OSI* using thin films. They showed that a finite degree of BOO persists well into the C phase indicating that the two phases are not thermodynamically distinct.

5.3.2 Spontaneous polarisation P_s

Fig. 5.4 is a plot of P_s vs. temperature for 8SI*. In the C* phase P_s increases slowly with decreasing temperature, but increases steeply at the transition to the I* phase. As to be expected this is accompanied by an increase in the coercive field. The X-ray measurements show that the transition is first order with a concomitant two-phase coexistence region. Since, as we shall see later, the switching times are also considerably different, in C* and I* phases, it is of interest to examine whether the

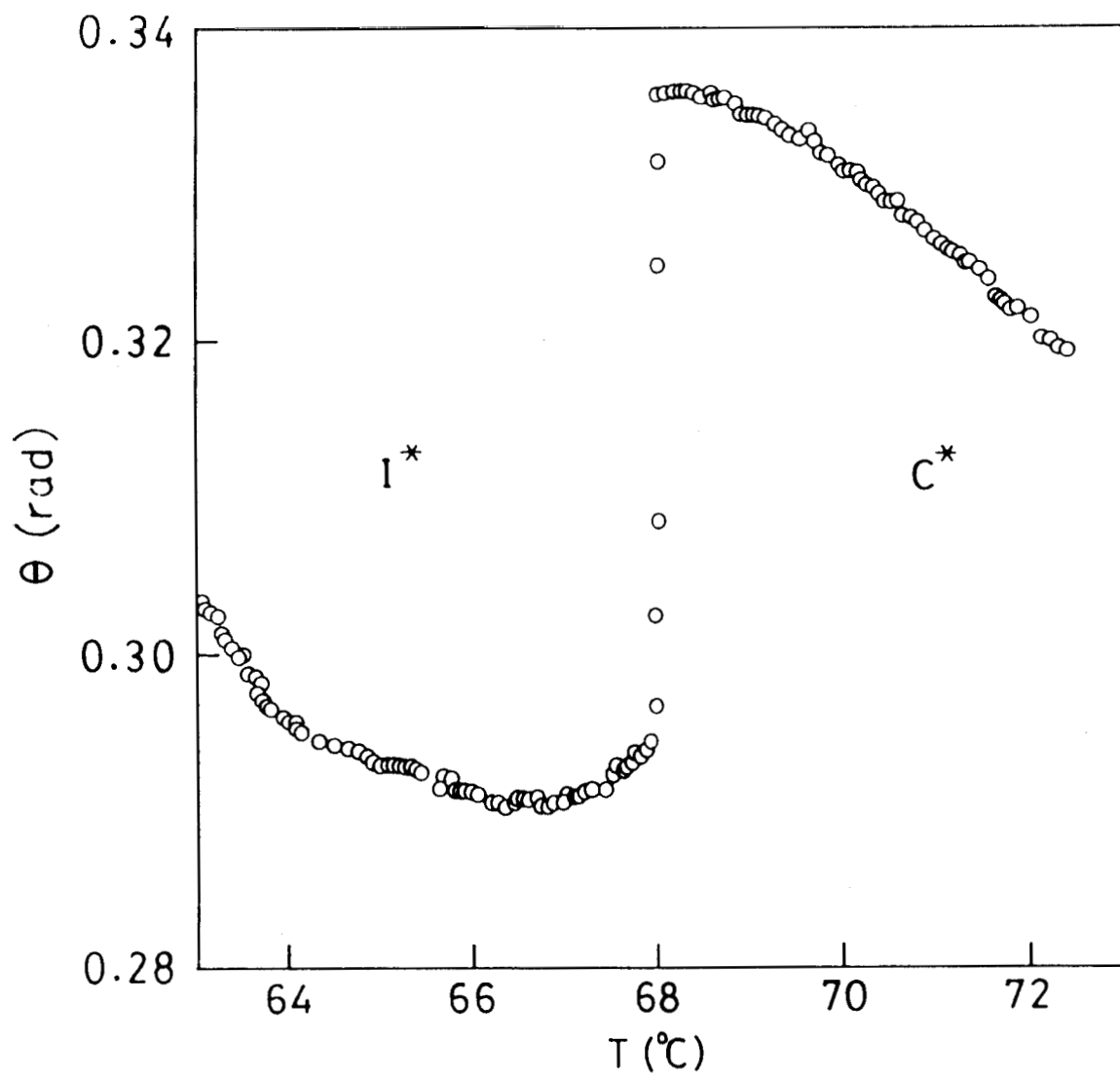


Fig.5.2. Temperature variation of the tilt angle for 8SI*.

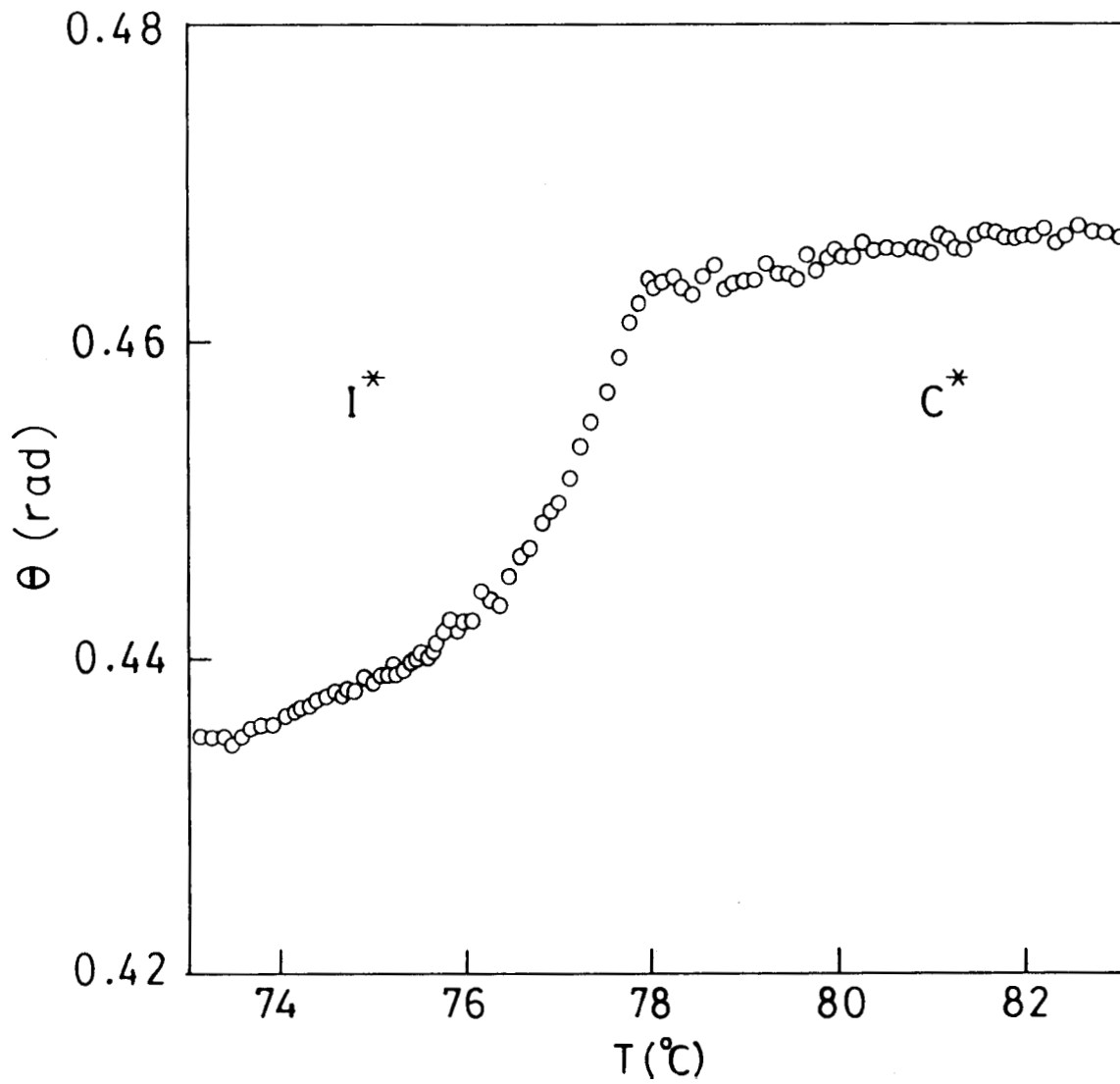


Fig.5.3. Temperature dependence of the tilt angle for 8OSI*.

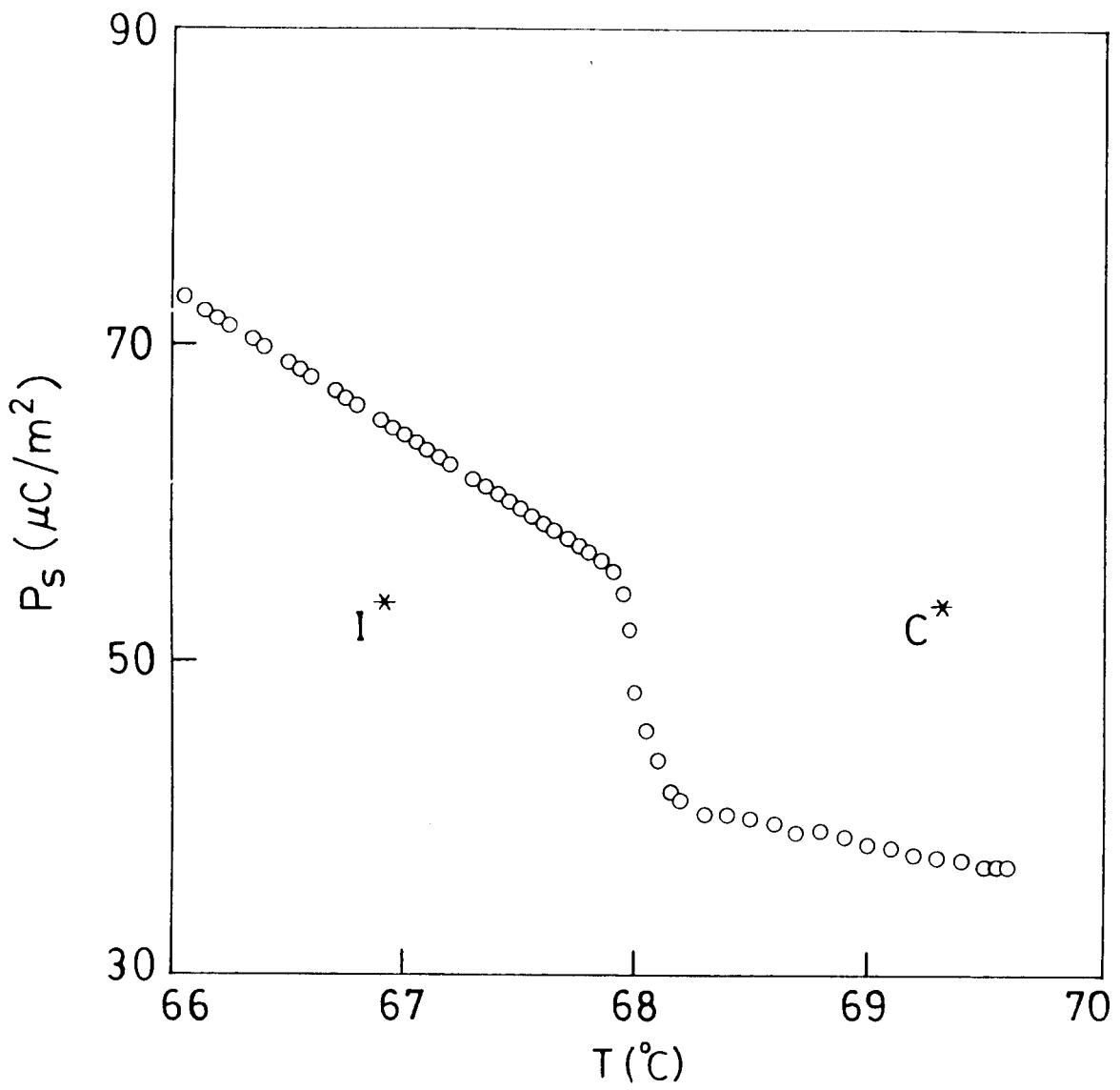


Fig.5.4. Temperature variation of P_s for 8SI*.

shape of the hysteresis loop gets altered in the two-phase region. Fig. 5.5a-c show the hysteresis loops obtained in the C^* phase at temperature 68.7°C , in the coexistence region at 67.5°C and at 63.9°C deep in the I^* phase respectively. The loops in Fig. 5.5a and 5.5c are single hysteresis loops. The pattern in Fig. 5.5b can be seen to be a combination of loops resulting out of a superposition of signals coming from coexistence domain belonging to the C^* and I^* phases and having different switching times. In fact one can observe the signal pattern varying continuously as one type of domain grows at the expense of the other on going through the coexistence region. It may be mentioned here that similar features were reported by Wahl and Jain⁸ in another compound exhibiting a first order C^* - I^* transition. In view of these observations, one may conclude that if such a **two** – loop pattern is observed in the transition region, then the transition is first order

The thermal variation of P_s for 8OSI^* is shown in Fig. 5.6 In the C^* phase close to the C^* - I^* transformation, P_s is more or less saturated just like the tilt angle. In the transition region, P_s starts decreasing in contrast to the behaviour of 8SI^* . Also, the hysteresis curves do not exhibit any "two-loop" pattern. This would mean that the transition is not first-order and that the I^* phase evolves continuously from the C^* phase without a phase transition. This is in agreement with the results of tilt angle measurements. However, similar to 8SI^* , the E_c value of SOSI^* increases on going to the I^* phase.

Comparing the plots of P_s and θ for 8OSI^* (Figs. 5.6 and 5.3), both P_s and θ decrease across the C^* - I^* transition. This indicates that P_s is proportional to θ not only in the C^* phase but also in the I^* phase. In fact it is known^{9,10} that in a vast majority of compounds the linear relationship between P_s and θ is maintained not only in the C^* phase, but also in the more highly ordered ferroelectric smectic

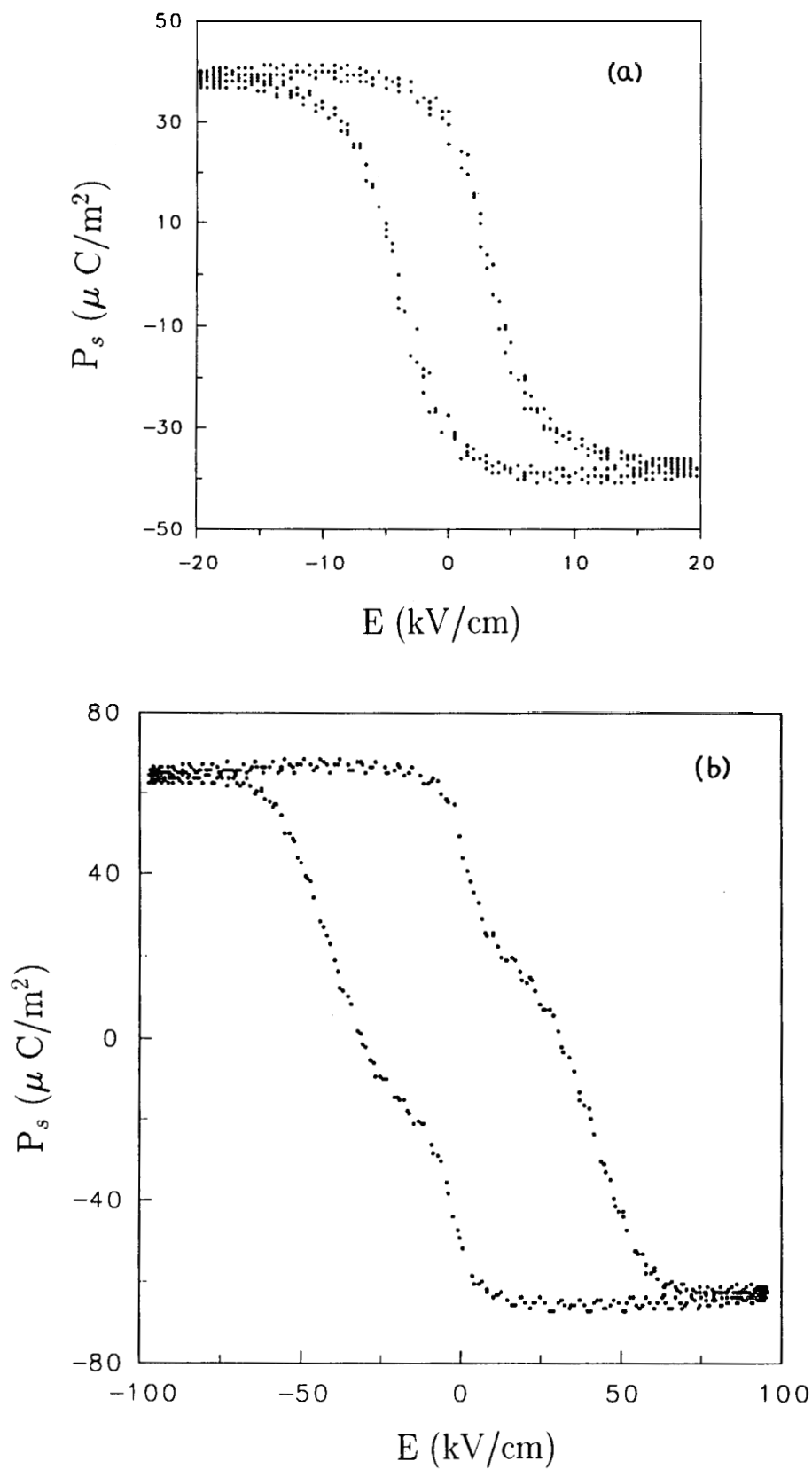
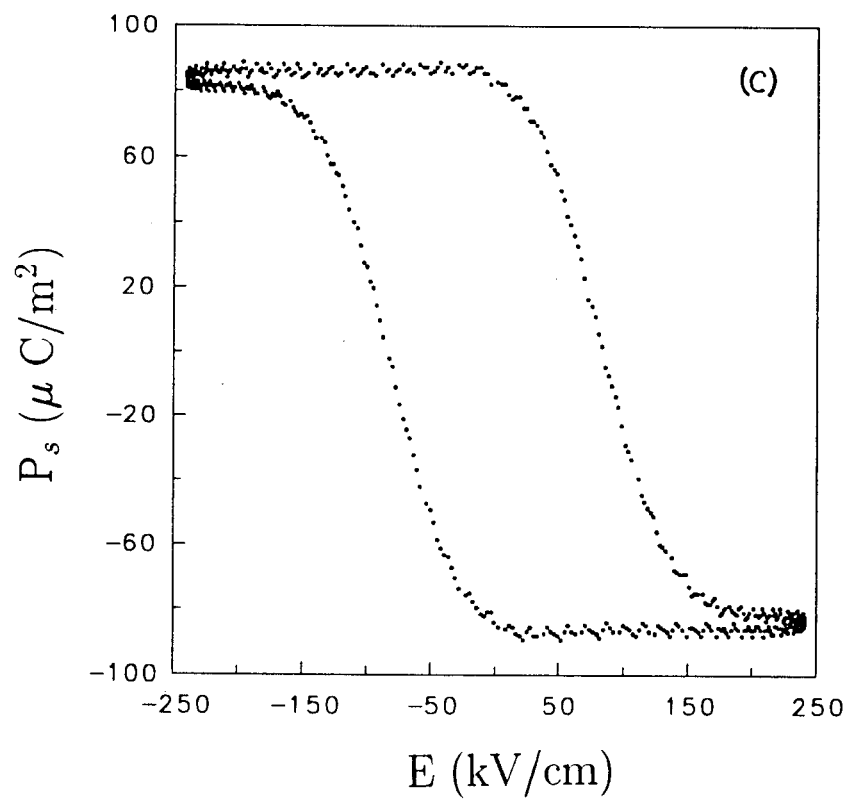


Fig.5.5. Representative hysteresis loops in the (a) C^* phase (68.7°C), (h) coexistence region (67.5°C), and (c) I^* phase (63.9°C).



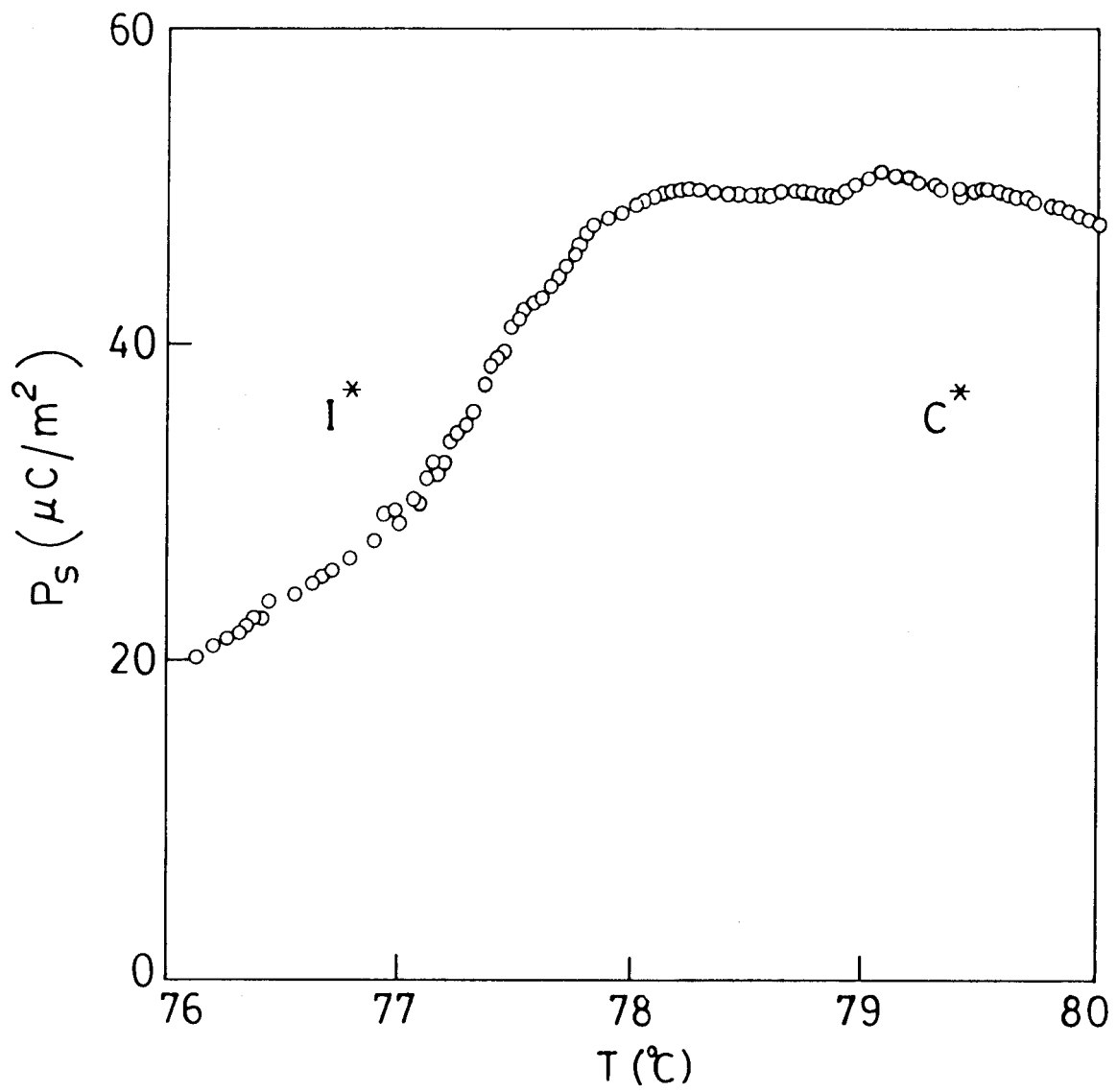


Fig.5.6. Temperature variation of P_s for 80SI*.

phases (I^* , $I^{*'} , \dots$). In this respect, the behaviour of $8SI^*$ is surprisingly different from that of $8OSI^*$. In $8SI^*$, though θ decreases in I^* phase (Fig. 5.2) the value of P_s increases rapidly and reaches a value, in I^* phase, which is double the value in the C^* phase. The reason for this rapid increase in P_s despite the decrease in θ may be due to an enormous increase in the rotational viscosity γ_ϕ in the I^* phase. To verify this, we have determined γ_ϕ as a function of temperature near the C^* - I^* transition by the hysteresis loop method¹¹ described in chapter IV. Fig. 5.7 is a plot of γ_ϕ vs. temperature for $8SI^*$. It is clearly seen from the figure that there is a jump in the value of γ_ϕ across the C^* - I^* transition and the value of γ_ϕ in the I^* phase is an order of magnitude larger than that in the C^* phase. Whereas the decrease in θ in the I^* phase is just 10%. This clearly explains the rapid increase in P_s despite the decrease in θ in the I^* phase.

Theories predict¹²⁻¹⁴ that due to the bilinear $P_s - \theta$ coupling the P_s is proportional to tilt, and measurements¹⁵ have shown that P_s/θ is weakly temperature dependent in the C^* phase away from the A- C^* transition temperature. To see whether this is valid in the I^* phase, we have plotted P_s/θ vs. temperature for the two compounds $8SI^*$ and $8OSI^*$ in figures 5.8 and 5.9 respectively. For both the compounds P_s/θ exhibits a strong temperature dependence in the I^* phase. The behaviour is similar to that of the thermal variation of P_s , suggesting that the P_s variation with temperature has a more dominant role than the θ variation near the C^* - I^* transition for both the materials.

In order to see whether the features seen in the thermal variation of θ , P_s and P_s/θ are reflected in the dielectric properties of the two compounds, we have measured the static dielectric constant ϵ_\perp for the two compounds. These measurements were performed at a frequency of 500 Hz, which is lower than the Goldstone mode

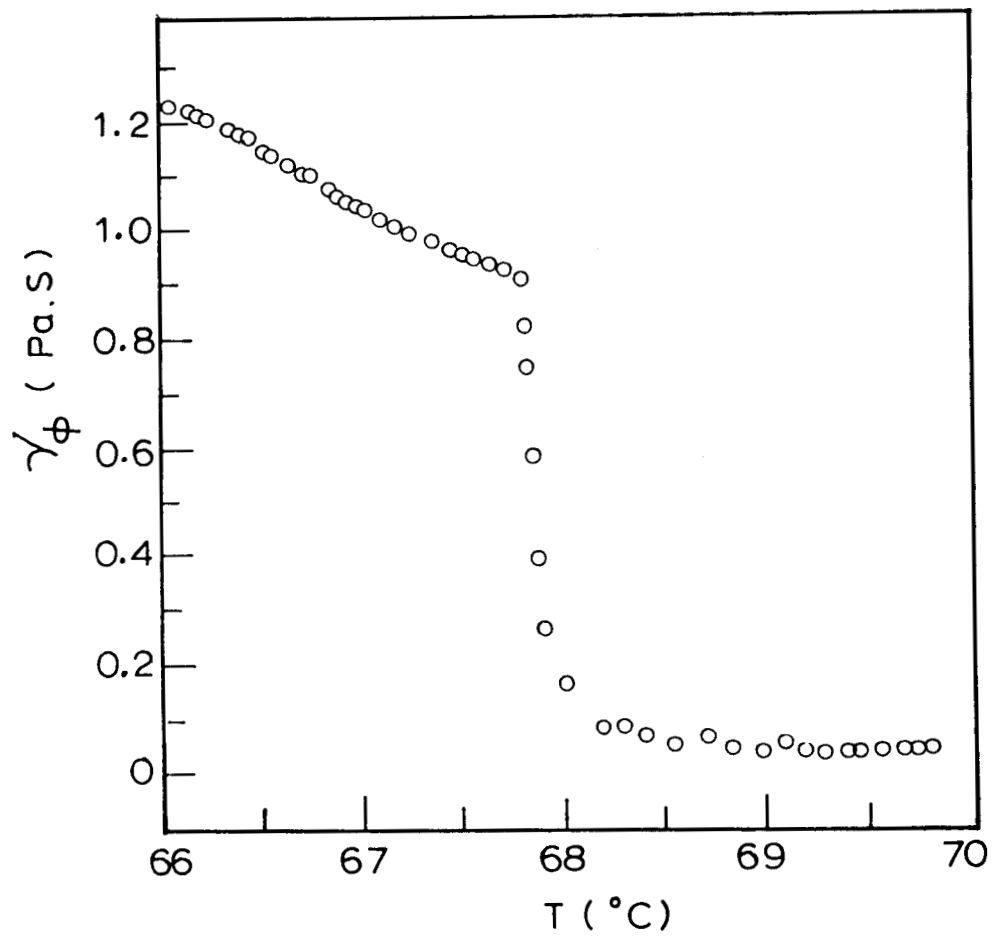


Fig.5.7. Temperature dependence of the rotational viscosity γ_ϕ for 8SI*.

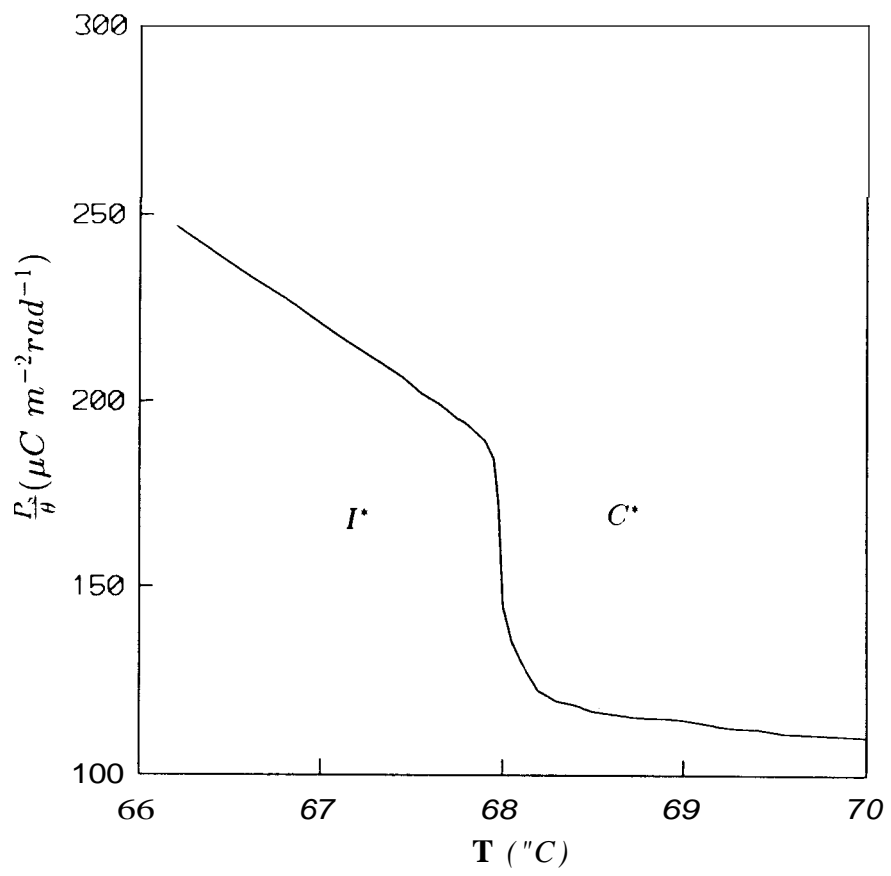


Fig.5.8. P_s/θ versus temperature for 8SI*.

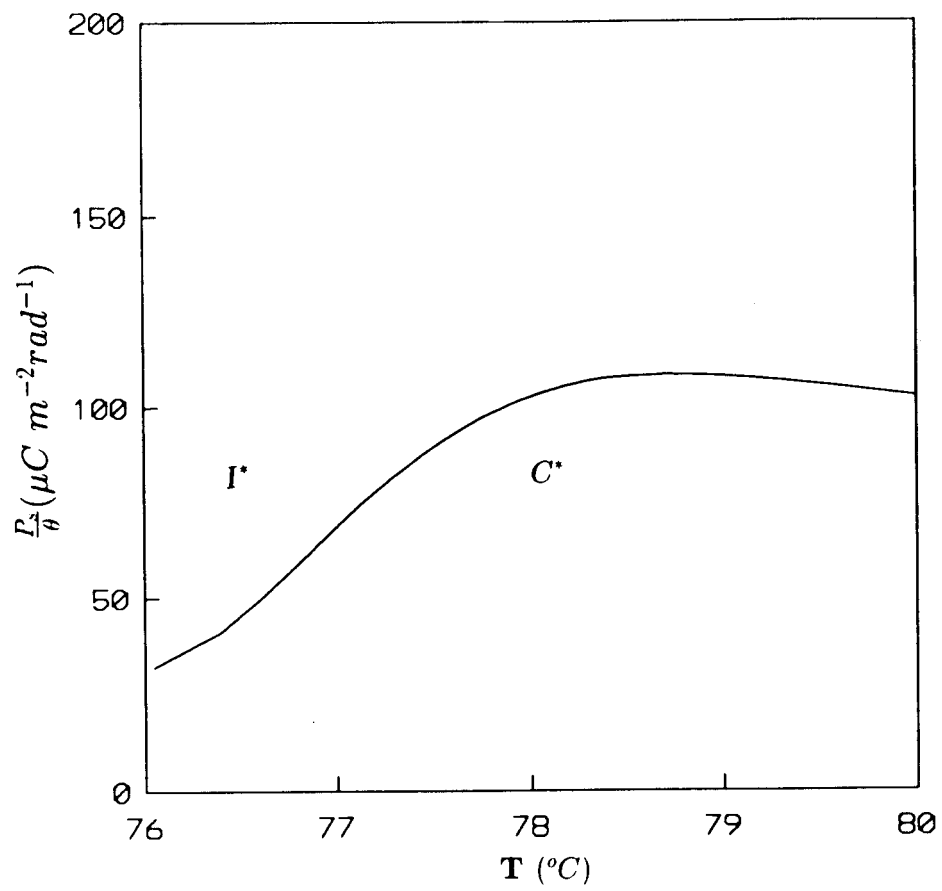


Fig.5.9. Temperature variation of the P_s/θ for 8OSI*.

frequency in the C* and I* phases of both the compounds^{16,17}. The plots of ϵ_{\perp} against temperature, for the two compounds, are shown in figures 5.10 and 5.11. This low-frequency dielectric constant, characterising the strength of the ferroelectric relaxation, shows dramatic decrease in the vicinity of the transition region. It is interesting to note that the drop in ϵ_{\perp} value is seen to be more for 8OSI* than for SSI*. From the mean field model¹⁵, one should expect the P_s/θ variation to be reflected in the temperature dependence of ϵ_{\perp} also, if other parameters like pitch, elastic constant, etc., remain unaltered. As we have seen earlier, for 8OSI* P_s/θ decreases in the I* phase and this explains the larger ϵ_{\perp} drop of 8OSI* at the C*-I* transition. However, this is not true for SSI* in which P_s/θ increases and one may expect an increase in the value of ϵ_{\perp} . But experimental measurements show that ϵ_{\perp} decreases for SSI* also. Thus to explain this ϵ_{\perp} variation with temperature for 8SI* one should consider the temperature dependence of pitch and elastic constants, as the strength of the Goldstone mode relaxation depends on these factors and is given by the relation¹⁸

$$\Delta\epsilon_G = \frac{1}{\epsilon_o 2K_3 q^2} \left(\frac{P_s}{\theta}\right)^2 \quad (5.1)$$

It is shown¹⁹ that for 8SI* the pitch increases (i.e., $1/q^2$ increases) across the C*-I* transition. It may also be recalled that for 8SI* the bend elastic constant was observed²⁰ to have a jump across C*-I* transition and increases on going to the I* phase. Therefore it appears that for 8SI*, the increase in P_s/θ and $1/q^2$ is balanced by a larger increase in the K_3 value. Therefore the ϵ_{\perp} does not show a larger drop in ϵ_{\perp} across the C*-I* transition. Evidently parameters, such as K_3, q other than P_s/θ are also important in order to explain the temperature variation of ϵ_{\perp} .

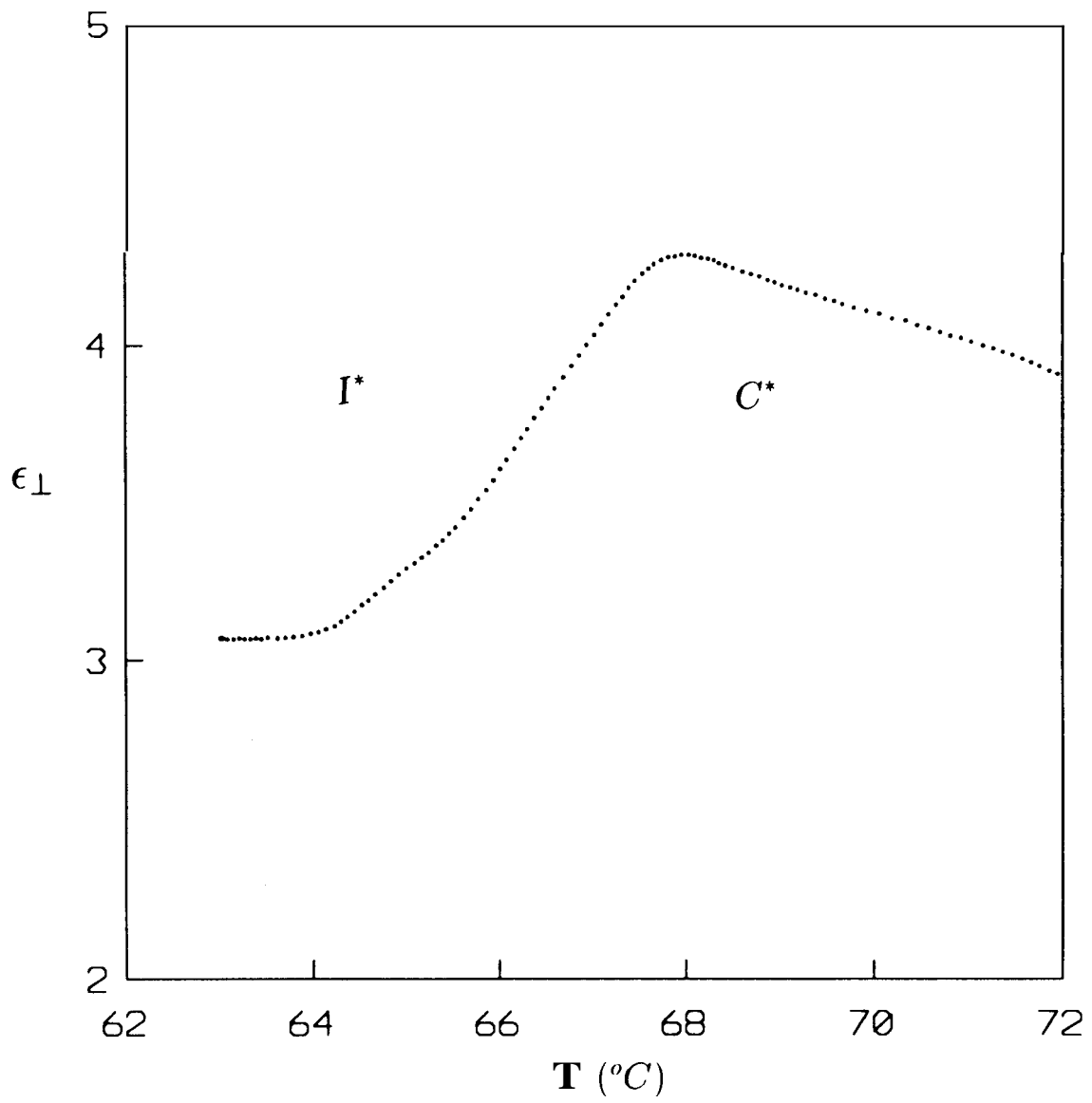


Fig.5.10. Temperature variation of ϵ_{\perp} for 8SI*.

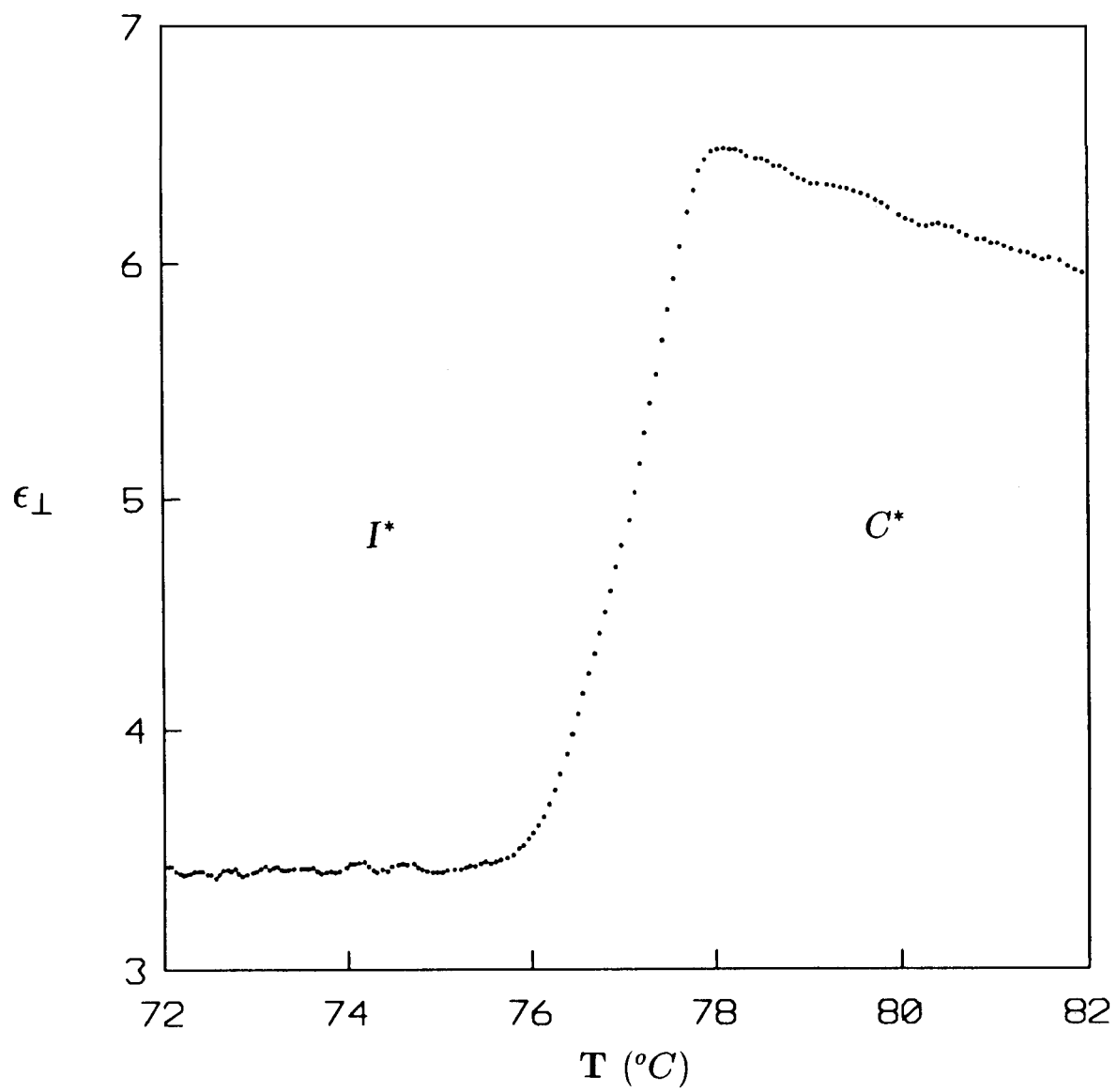


Fig.5.11. Temperature variation of ϵ_{\perp} for 80SI*.

References

- [1] S. Chandrasekhar, *Contemp. Phys.*, 29, 527 (1988).
- [2] A.J.Leadbetter, in *Thermotropic Liquid Crystals*, ed. G.W.Gray, *Critical Reports on Applied Chemistry*, Vol. 22 (John-Wiley & Sons, 1987).
- [3] J.D.Brock, A.Aharony, R.J.Birgeneau, K.W.Evans-Lutterodt, J.D.Litster, P.M.Horn, G.B.Stephenson and A.R.Tajbakhsh, *Phys. Rev. Lett.*, **57**, 98(1986).
- [4] J.D.Brock, D.Y.Noh, B.R.McClain, J.D.Litster, R.J.Birgeneau, A.Aharony, P.M.Horn, and J.C.Liang, *Z. Phys.*, **B74**, 157 (1989).
- [5] D.R.Nelson and B.I.Halperin, *Phys. Rev.*, B 21, 5312 (1980).
- [6] B.Zeks, T.Carlsson, C.Filipic and B.Urbanc, *Ferroelectrics*, 84, 3 (1988).
- [7] Both the compounds were kindly provided to us by BDH (Poole) Ltd.
- [8] H.Diamant, K.Drenck and R.Pepinsky, *Rev.Sci.Instrum.*, 28, 30(1957).
- [9] J.Wahl and S.C.Jain, *Ferroelectrics*, **58**, 481(1984).
- [10] R.Eidenschink, T.Geelhaar, G.Andersson, A.Dahlgren, K.Flatschler, F.Gouda, S.T.Lagerwall and K.Skarp, *Ferroelectrics*, 84, 167 (1988).
- [11] C.Escher, H.R.Dubal, W.Hemmerling, I.Muller, D.Ohlendorf and R.Wingen, *Ferroelectrics*, 84, 89(1988).
- [12] B.Zeks, T.Carlsson, C.Filipic and B.Urbanc, *Ferroelectrics*, 84, 3 (1988)
- [13] R.Blinc and B.Zeks, *Phys. Rev.*, **A18**, 740 (1978)
- [14] L.G.Benguigi, *Ferroelectrics*, **58**, 269 (1984).

- [15] S.Dumrongrattana and C.C.Huang, *Phys. Rev. Lett.*, **56**, 464 (1986).
- [16] R.J.Cava, J.S.Patel and E.A.Rietman, *J.Appl.Phys.*, **60**, 3093(1986).
- [17] M.Pfeiffer, S.Wrobel, L.A.Beresnev and W.Haase, *Mol. Cryst. Liquid Cryst.*, **202**, 193 (1991).
- [18] C.Filipic, T.Carlsson, A.Levstik, B.Zeks, R.Blinc, F.Gouda, S.T.Lagerwall and K.Skarp, *Phys. Rev.*, **A38**, 5833 (1988).
- [19] W. Kuczynski and H.Stegemeyer, *Liquid Crystals*, **5**, 553 (1989).
- [20] S.B.Dierker and R.Pindak, *Phys. Rev. Lett.*, **55**, 1002 (1987).